

# Organometallic Chemistry of Ga<sup>+</sup>: Formation of an Unusual Gallium Dimer in the Coordination Sphere of Ruthenium\*\*

Thomas Cadenbach,<sup>[a]</sup> Christian Gemel,<sup>[a]</sup> Timo Bollermann,<sup>[a]</sup> Israel Fernandez,<sup>[b]</sup> Gernot Frenking,<sup>[c]</sup> and Roland A. Fischer\*<sup>[a]</sup>

In memoriam our dear friend and colleague Beatrice Buchin

**Abstract:** New insights into the distinct organometallic chemistry of the Ga<sup>+</sup> ion are presented. Ga<sup>+</sup> reacts as a strong electrophile with the electron rich ligand trismethylene-methane (C(CH<sub>2</sub>)<sub>3</sub><sup>2-</sup>) attached at Ru by insertion into a Ru–C bond. The resulting “gal-lamethylallyl” ligand behaves like strong nucleophile similar to known monovalent GaR species. This donor property leads to the dimeric structure of the product  $[\{\text{Ru}(\text{GaCp}^*)_3-$

$[\eta^3-(\text{CH}_2)_2\text{C}\{\text{CH}_2(\mu\text{-Ga})\}\}_2][(\text{BAR}^{\text{F}})_2]$  (**4**) (Cp\* = C<sub>5</sub>Me<sub>5</sub>, [BAR<sup>F</sup>] = [B{C<sub>6</sub>H<sub>3</sub>(CF<sub>3</sub>)<sub>2</sub>]<sub>4</sub>)). Very unexpectedly, the two gallium ligands in this dimer are found in close vicinity to each other with a distance in the range of Ga–Ga bonds.

**Keywords:** density functional calculations • gallium • low-valent ion • metal–metal interactions • ruthenium

Indeed, AIM calculations confirm a weak attractive closed shell Ga–Ga interaction. Finally, a novel example of a complex with substituent-free Ga<sup>+</sup> as a ligand was found in the compound  $[\text{Ru}(\text{PCy}_3)_2(\text{GaCp}^*)_2(\text{Ga})][\text{BAR}^{\text{F}}]$  (**6**) (Cy = C<sub>6</sub>H<sub>11</sub>, cyclohexyl), the very short Ru–Ga bond length confirming the assumption that Ga<sup>+</sup> represents a pure σ/π-accepting ligand in this case.

## Introduction

The concept of kinetic stabilization of monovalent group 13 compounds ER by the use of very bulky substituents (e.g. Cp\*, substituted terphenyl- or bisimidate ligands) has led to a rich chemistry.<sup>[1–8]</sup> Quite recently, it was reported that even sterically not shielded and thus elusive species such as

GaI<sup>[9]</sup> and GaCH<sub>3</sub><sup>[10]</sup> can be trapped as terminal ligands in the coordination sphere of transition metal centers. Obviously, the ultimate limit in this series is the chemistry of naked, substituent-free Ga<sup>+</sup>.<sup>[11]</sup> Indeed, the reaction of  $[\text{Ga}_2\text{Cp}^*][\text{BAR}^{\text{F}}]$  (Cp\* = C<sub>5</sub>Me<sub>5</sub>, [BAR<sup>F</sup>] = [B{C<sub>6</sub>H<sub>3</sub>(CF<sub>3</sub>)<sub>2</sub>]<sub>4</sub>) with the electron rich 18 valence electron (VE) complexes  $[\text{PtL}_4]$  (L = PR<sub>3</sub>, GaCp\*) leads to  $[\text{L}_4\text{PtGa}]^+$ , which displays terminally bound Ga<sup>+</sup> ions.<sup>[12–14]</sup> density functional theory (DFT) calculations confirm the nature of the Pt–Ga interaction as weakly polar donor-acceptor bond with the Ga<sup>+</sup> ion acting as strong σ- and π-acceptor without any donor properties, that is, the s-type free electron pair of Ga<sup>+</sup> is sterically and chemically not active. One may call the donor properties for Ga<sup>+</sup> as “switched off” in this situation. A distinctive organometallic chemistry of Ga<sup>+</sup>, however, has not been investigated so far. The major problem with Ga<sup>+</sup> is the tremendous redox lability, being easily reduced or oxidized by many reaction partners including redox-active transition metal centers. Nevertheless, we regard naked Ga<sup>+</sup> as a very interesting synthon for unusual complexes of the type  $[\text{L}_n\text{M–GaR}']$  (M = transition metal, R' = anionic ligand, other than Cp\*, etc.), for example, by insertion of Ga<sup>+</sup> into M–R' bonds or by addition of nucleophilic fragments R' to electrophilic  $[\text{L}_n\text{MGa}]^+$  complexes. Although such reactions

[a] T. Cadenbach, Dr. C. Gemel, T. Bollermann, Prof. R. A. Fischer  
Inorganic Chemistry II—Organometallics & Materials  
Faculty of Chemistry and Biochemistry  
Ruhr University Bochum, 44870 Bochum (Germany)  
Fax: (+49) 234-321-4174  
E-mail: roland.fischer@rub.de

[b] Dr. I. Fernandez  
Dpto. Química Orgánica, Facultad de Química  
Universidad Complutense de Madrid, 28040 Madrid (Spain)

[c] Prof. G. Frenking  
Department of Chemistry  
Philipps-University Marburg, 35032 Marburg (Germany)

[\*\*] Organo group 13 complexes of d-block elements LIV, for LIII see ref. [17]

Supporting information for this article is available on the WWW under <http://dx.doi.org/10.1002/chem.200801328>.

are unknown for  $\text{Ga}^+$  so far, many examples exist of insertion reactions of neutral GaR species more or less always leading to complexes of the type  $[\text{L}_n\text{M}-\text{GaXR}]$ .<sup>[10,15–19]</sup> Exceptions from this general reaction are known, for example, for starting complexes bearing two (or potentially more) anionic groups X, leading to formation of the  $\text{Ga}^{\text{III}}$  side product  $\text{RGaX}_2$  and thus reduction of the transition metal center. A recent example for this would be the reduction of  $\text{SnCl}_2$  by the beta-diketiminato  $\text{Ga}(\text{DDP})$  ( $\text{DDP} = \text{HC}(\text{CMeHC}_6\text{H}_3-2,6-i\text{Pr}_2)_2$ ) leading to the unusual gallium-ligand stabilized metalloid tin cluster  $[\text{Sn}_{17}\{\text{Ga}(\text{DDP})\text{Cl}\}_4]$ .<sup>[20]</sup> Along these lines, we wish to address two major questions concerning the organometallic reactivity of the cation  $\text{Ga}^+$  in this report: First, if  $\text{Ga}^+$  behaves as a strong electrophile towards Lewis basic transition metal centers, how about its behavior towards nucleophilic  $\pi$ -ligands? Secondly, what can we tell about its reactivity towards M–X motifs, taking into account the numerous examples of reactions of GaR with complexes  $[\text{L}_n\text{M}-\text{X}]$ ? As starting points for these reactivity studies of  $\text{Ga}^+$  towards organometallic substrates we chose the 18 VE complex  $[\text{Ru}(\text{GaCp}^*)_3(\text{TMM})]$  (**1**) ( $\text{TMM} = \eta^4\text{-C}(\text{CH}_2)_3$ ) as an example for a transition metal complex bearing the strongly  $\pi$ -donating ligand trimethylenemethane as well as  $[\text{Ru}(\text{PCy}_3)_2(\text{GaCp}^*)_2(\text{H})_2]$  (**2**) as a complex featuring two potentially reactive M–H bonds.

## Results and Discussion

**Synthesis and characterization of  $[\text{Ru}(\text{GaCp}^*)_3(\text{TMM})]$  (**1**) and  $[\text{Ru}(\text{PCy}_3)_2(\text{GaCp}^*)_2(\text{H})_2]$  (**2**):** First, we describe the preparation characterization of the two new compounds  $[\text{Ru}(\text{GaCp}^*)_3(\text{TMM})]$  (**1**) and  $[\text{Ru}(\text{PCy}_3)_2(\text{GaCp}^*)_2(\text{H})_2]$  (**2**), which are the starting materials for the study below. As for complex **1**, the reaction of the octahedral  $\text{Ru}^{\text{II}}$  starting complex  $[\text{Ru}(\eta^4\text{-COD})(\eta^3\text{-CH}_2\text{CMeCH}_2)_2]$ <sup>[21]</sup> ( $\text{COD} = \text{cyclooctadiene}$ ) with three molar equivalents of  $\text{GaCp}^*$  in toluene at  $80^\circ\text{C}$ , cleanly leads to  $[\text{Ru}(\text{GaCp}^*)_3(\text{TMM})]$  (**1**) in a yield of 62% within 1 hour. The formation of a TMM ligand by hydrogen transfer from a coordinated 2-methylallyl moiety is well known and has been described in literature in numerous examples.<sup>[22]</sup> The analysis of the  $^1\text{H}$  NMR and  $^{13}\text{C}$  spectra is in agreement with the proposed structure, and features signals for the TMM ligand at  $\delta = 1.76$  ppm (6H) in the  $^1\text{H}$  NMR spectrum and at  $\delta = 84.1$  (central carbon) and  $\delta = 24.5$  ppm ( $\text{CH}_2$ ) in the  $^{13}\text{C}$  NMR spectrum, respectively. The solid-state structure of **1** has been determined by a single crystal X-ray diffraction experiment. A POVray plot of **1** is shown in Figure 1 and important crystallographic data are summarized in Table S1 (see the Supporting Information). The umbrella-like puckering of the TMM ligand is usually quantified in terms of the angle  $\theta$ , which is measured to be  $12.0^\circ$  for **1**. This value matches well with the data of most other TMM complexes.<sup>[22,23]</sup> The Ru–Ga bond length averages to 2.348 Å, which is relatively short, but still in line with known  $\text{Ru}^{\text{II}}\text{–GaCp}^*$  complexes that also show symmetrically  $\eta^5$ -coordinated  $\text{Cp}^*$  ligands at the Ga centre.<sup>[16,19]</sup> The

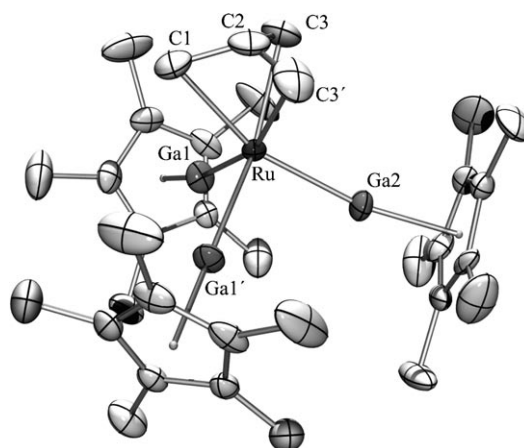


Figure 1. Molecular structure of  $[\text{Ru}(\text{GaCp}^*)_3(\text{TMM})]$  **1** in the solid state as determined by X-ray single crystal diffraction (thermal ellipsoids are shown at the 50% probability level, hydrogen atoms have been omitted for clarity).

preparation of the second test complex, the  $\text{Ru}^{\text{II}}$  hydride,  $[\text{Ru}(\text{PCy}_3)_2(\text{GaCp}^*)_2(\text{H})_2]$  (**2**) starts out from Chaudret's ruthenium polyhydride  $[\text{Ru}(\text{PCy}_3)_2(\text{H})_2(\text{H})_2]$  ( $\text{Cy} = \text{C}_6\text{H}_{11}$ , cyclohexyl).<sup>[24]</sup> Reaction of a freshly prepared sample of this complex with two equivalents of  $\text{GaCp}^*$  in hexane results in evolution of  $\text{H}_2$  and formation of **2** in high yield. The hydride signal appears at  $\delta = -12.74$  ppm in the  $^1\text{H}$  NMR spectrum as a triplet due to coupling with the  $\text{PCy}_3$  ligands indicating that  $\text{PCy}_3$  does not dissociate in solution. The shift of the hydride signal is well in agreement with terminal Ru–H complexes reported in literature.<sup>[25–27]</sup>

In addition, the transversal relaxation time  $T_1$  of **2** has been determined to be above 300 ms, which clearly indicates the classical dihydride structure of **2**.<sup>[28,29]</sup> Single crystals suitable for X-ray diffraction studies, were obtained by slowly cooling a saturated pentane solution of **2** down to  $-30^\circ\text{C}$  for several days. Important crystallographic data are summarized in Table S1 (see the Supporting Information) and the molecular structure is shown in Figure 2. Compound **2** crystallizes in the monoclinic space group  $P2(1)/c$  with two almost identical molecules in the asymmetric unit. The hydride ligands were located in the course of the refinement of the solid state structure. The presence of terminal hydride ligands in the solid state structure of **2** is further substantiated by IR spectroscopy which reveals two sharp absorptions in the typical region for terminal ruthenium hydride ligands ( $\tilde{\nu} = 2026$  and  $2002\text{ cm}^{-1}$ ). The coordination geometry around the metal center is described as a distorted octahedron defined by the two axial phosphines in the *trans* position, two  $\text{GaCp}^*$  ligands are *cis* to each other and two hydrides are *trans* to the  $\text{GaCp}^*$  moieties. As already observed in similar complexes,<sup>[30,31]</sup> the phosphorous atoms are bent towards the hydride ligands resulting in a P2–Ru–P1 angle of  $145.54(4)^\circ$ . The angle between the  $\text{GaCp}^*$  ligands is about  $94.67(2)^\circ$  and the Ru–Ga bond lengths (Ru1–Ga1 =  $2.4019(7)$  Å and Ru1–Ga2 =  $2.4014(7)$  Å) are in the range of other Ru– $\text{GaCp}^*$  complexes. The  $\text{Cp}^*$  groups are clearly

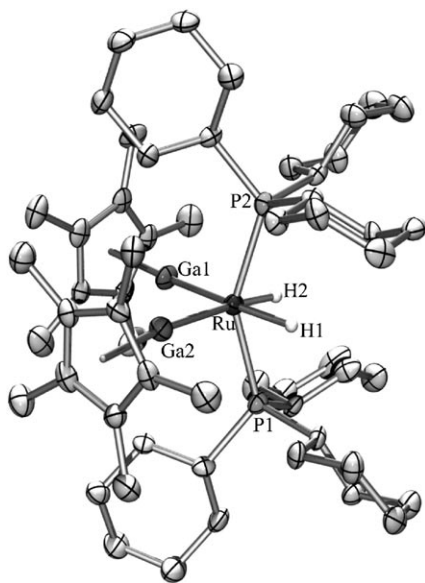


Figure 2. Molecular structure of  $[\text{Ru}(\text{PCy}_3)_2(\text{GaCp}^*)_2(\text{H})_2]$  **2** in the solid state as determined by X-ray single crystal diffraction (thermal ellipsoids are shown at the 50% probability level, hydrogen atoms except H1 and H2 have been omitted for clarity).

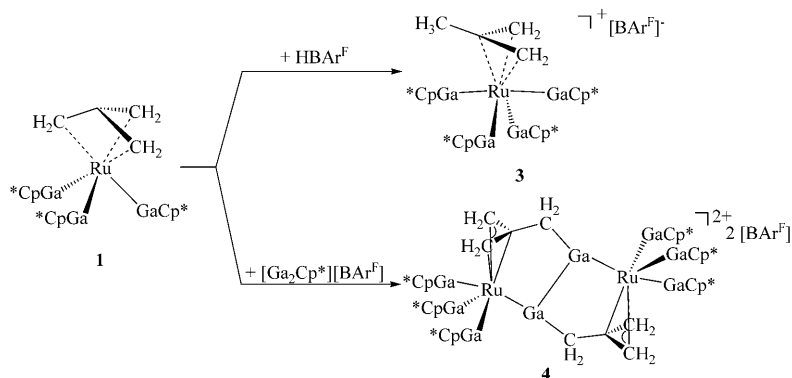
$\eta^5$ -bound to the Ga atoms ( $\text{Ga1-Cp}^*_{\text{centr}}$  2.046 Å,  $\text{Ga2-Cp}^*_{\text{centr}}$  2.053 Å), and do not exhibit any unusual features.

It should be noted, that a reaction analogous to the synthesis of **2** that uses  $\text{AlCp}^*$  instead of  $\text{GaCp}^*$  clearly leads to the related complex  $[\text{Ru}(\text{PCy}_3)(\text{AlCp}^*)_2(\text{H})_2]$  bearing one  $\text{PCy}_3$  ligand less than the gallium complex **2**. Analysis of the  $^1\text{H}$  and  $^{13}\text{C}$ , as well as  $^{31}\text{P}$  NMR spectra, of the reaction product leads to a very good agreement with the proposed 16 VE structure, however, the separation of the liberated  $\text{PCy}_3$  and the isolation of the aluminum complex in pure form were unsuccessful. Therefore, neither elemental analysis nor single crystal X-ray structural analysis of this complex could be performed.

**The addition of  $\text{H}^+$  and  $\text{Ga}^+$  to  $[\text{Ru}(\text{GaCp}^*)_3(\text{TMM})]$  (**1**):** The bis-allyl type TMM ligand represents a strongly stabilizing, yet potentially reactive organometallic co-ligand and, therefore, **1** seemed to be a good candidate to study the reactivity of the  $\text{Ga}^+$  ion. As  $\text{Ga}^+$  is a strong Lewis acid, similar to  $\text{H}^+$ ,<sup>[12]</sup> we first studied the protonation of **1** by  $[\text{H}(\text{OEt}_2)_2][\text{BAR}^{\text{F}}]$  and consequently obtained  $[\text{Ru}(\text{GaCp}^*)_4\{\eta^3\text{-(CH}_2)_2\text{C(CH}_3)\}][\text{BAR}^{\text{F}}]$  (**3**) in good yield of about 60–70% (Scheme 1). The selectivity of the reaction is high, no organometallic by-products were detected by in situ NMR spectroscopy. In particular, protolysis of a  $\text{Cp}^*$  group was not observed. This is in sharp contrast to  $[\text{Rh}(\text{Cp}^*\text{Ga})_4(\eta^1\text{-}$

$\text{Cp}^*\text{GaCH}_3)$ ], which reacted with  $[\text{H}(\text{OEt}_2)_2][\text{BAR}^{\text{F}}]$  by liberation of  $\text{Cp}^*\text{H}$  to yield the first terminally coordinated  $\text{GaMe}$  species, namely  $[\text{Rh}(\text{Cp}^*\text{Ga})_4(\text{GaCH}_3)][\text{BAR}^{\text{F}}]$ .<sup>[10]</sup> This result shows that the most nucleophilic site in **1** is indeed the TMM ligand. The formation of a  $\eta^3\text{-}\pi$ -allylic ligand by protonation of the  $\eta^4\text{-}\pi$ -allylic TMM suggests that only a small fraction of the  $\pi$ -bond energy is lost, which certainly contributes to the overall driving force of the reaction. The exact origin of the fourth equivalent of  $\text{GaCp}^*$  in **2** which saturates the formal 18 VE count of the ruthenium center is unclear, so far. Some decomposition of the starting complex **1** on protonation under liberation of  $\text{GaCp}^*$  is likely. Analysis of the  $^1\text{H}$  as well as  $^{13}\text{C}$  NMR spectra is in good agreement with the proposed structure of **3**, with three signals at  $\delta = 2.52$  (d, *syn*-H),  $\delta = 2.29$  (d, *anti*-H) and  $\delta = 2.11$  ppm (s,  $\text{CH}_3$ ) for the methylallyl ligand.

Upon slow diffusion of *n*-hexane into a THF solution of **3** at room temperature, pale yellow single crystals were isolated. A single crystal X-ray diffraction study reveals a distorted octahedral structure for the cation  $[\text{Ru}(\text{GaCp}^*)_4\{\eta^3\text{-(CH}_2)_2\text{C(CH}_3)\}]^+$  (Figure 3, see Table S1 in the Supporting Information for details of the analysis). Two  $\text{GaCp}^*$  li-



Scheme 1. Reaction of **1** with  $[\text{H}(\text{OEt}_2)_2][\text{BAR}^{\text{F}}]$  and  $[\text{Ga}_2\text{Cp}^*][\text{BAR}^{\text{F}}]$  in fluorobenzene solution.

gands occupy the axial positions ( $\text{Ga2-Ru1-Ga4}$  *trans*-angle of  $172.93(2)^\circ$ ), whereas the remaining two  $\text{GaCp}^*$  ligands are localized in the equatorial plane *trans* to the methylallyl group ( $\text{Ga1-Ru1-Ga3}$  *cis*-angle of  $99.09(2)^\circ$ ). The Ru–Ga bond lengths range from 2.3848(6) Å for Ru1–Ga2 to 2.4433(6) Å for Ru1–Ga4 with an average value of 2.412 Å and are, therefore, elongated by 2.7% compared to the starting complex  $[\text{Ru}(\text{GaCp}^*)_3(\text{TMM})]$  (**1**). The  $\text{Cp}^*$  groups of each low-valent group 13 ligand are in a clear  $\eta^5$  binding mode with  $\text{Ga-Cp}^*_{\text{centr}}$  bond lengths of 1.960–1.995 Å (average 1.977 Å). Notably, the  $\text{Cp}^*$  group bound to Ga4 is significantly bent to the equatorial plane resulting in an angle Ru–Ga4– $\text{Cp}^*_{\text{centr}}$  of  $150.57^\circ$ . The methylallyl ligand is characterized by a typical  $\eta^3$  coordination mode with C–C and Ru–C bond lengths similar to those of reported ruthenium allyl complexes.<sup>[32–37]</sup>

In analogy to the addition of  $\text{H}^+$ , we treated of **1** with one molar equivalent of the  $\text{Ga}^+$  transfer reagent  $[\text{Ga}_2\text{Cp}^*]\text{-}$

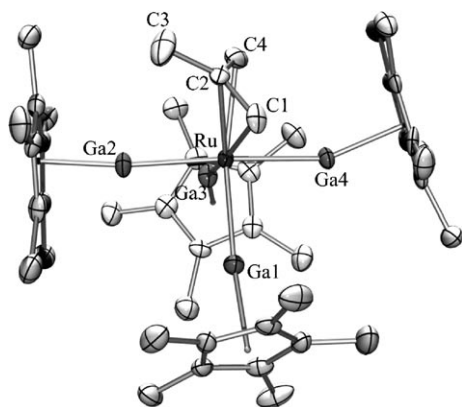


Figure 3. Molecular structure of the cationic part of **3** in the solid state as determined by X-ray single crystal diffraction (thermal ellipsoids are shown at the 50% probability level, hydrogen atoms have been omitted for clarity).

[BAR<sup>F</sup>] in fluorobenzene at room temperature. Subsequent crystallization by means of slow diffusion of *n*-hexane into this solution at 25 °C afforded air sensitive deep red crystals of  $[\{\text{Ru}(\text{GaCp}^*)_3[\eta^3\text{-(CH}_2)_2\text{C}\{\text{CH}_2(\mu\text{-Ga})\}]\}_2][(\text{BAR}^F)_2]$  (**4**) in a preparative yield of  $\geq 80\%$  (Scheme 1). Complex **4** is stable in the solid state, but isomerizes in polar solvents such as fluorobenzene at elevated temperature (vide infra). In the solid state structure of **4** (Figure 4), both ruthenium centers are coordinated in a distorted octahedral environment. A “gallamethylallyl” fragment, in which one proton of the methyl group of a methylallyl ligand is replaced by a gallium atom, coordinates in the equatorial plane of each ruthenium center *trans* to two GaCp\* ligands. The gallium atom of the gallamethylallyl ligand is coordinated at the adjacent ruthenium center and is therefore part of its axial environment which is completed by a third GaCp\* ligand. The

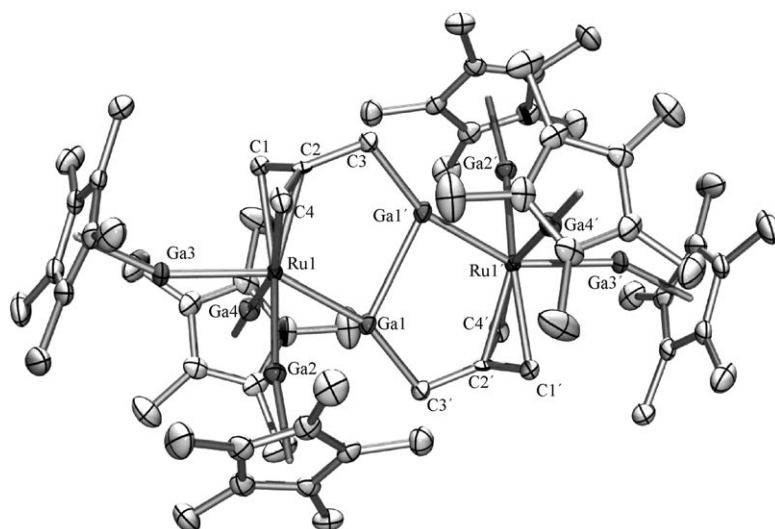


Figure 4. Molecular structure of the cationic part of **4** in the solid state as determined by X-ray single crystal diffraction (thermal ellipsoids are shown at the 50% probability level, hydrogen atoms have been omitted for clarity).

Ga1–C3 bond length of 1.959(3) Å is almost identical to the reported Ga–CH<sub>3</sub> bond length in the isoelectronic and structurally related complex  $[\text{Rh}(\text{GaCp}^*)_4(\text{GaCH}_3)][\text{BAR}^F]$  (Ga–CH<sub>3</sub> 1.958(11) Å).<sup>[10]</sup> The most striking feature of **3** is the short Ga1–Ga1' length of 2.5836(8) Å. Comparable lengths are found in Ga<sup>I</sup> clusters (e.g. 2.568 Å in  $[\text{Ga}_4\text{(Si}t\text{Bu}_3)_4]$ <sup>[38]</sup>) or Ga<sup>II</sup>–Ga<sup>II</sup> dimers (e.g. 2.515 Å in  $[\text{Ga}_2\text{(C}_6\text{H}_2i\text{Pr}_3)_4]$ ).<sup>[39]</sup>

Interestingly, compound **3** undergoes an irreversible thermal isomerization upon prolonged heating (Figure 5). When a pure crystalline sample of **3** was refluxed in fluorobenzene for 30 min at 85 °C a color change from dark red to pale yellow took place. Upon slow diffusion of *n*-hexane into this solution at 25 °C, pale-yellow single crystals of the salt  $[\{\text{Ru}(\text{GaCp}^*)_3[\eta^3\text{-(CH}_2)_2\text{C}\{\text{CH}(\mu\text{-Ga})(\text{CH}_3)\}]\}_2][(\text{BAR}^F)_2]$  (**5**) were isolated in 91% yield. The molecular structure of **5** was determined by X-ray analysis (Figure 5, Table S1) and is very similar to that of **4** (Figure 3). However, in **5** the gallium atom is no longer bound to an *aliphatic* CH<sub>2</sub> group, but rather to a *vinyl* group, that is, the terminal carbon of the allylic unit. Thus the thermal isomerization **4**→**5** can be viewed as a “tautomerism” of the allyl fragment. As a result of this rearrangement the Ru1–Ga1 length 2.3920 Å is slightly elongated compared to **4** whereas the corresponding Ru1–Ga5 (2.8734 Å) as well as the Ga1→Ga5 (2.5399 Å) bonds are slightly shortened. Interesting features of both isomers **4** and **5** are the angles Ru1–Ga1–C3' of 159.0(1)° and Ru1–Ga1–C37 and Ru2–Ga5–C3 of 171.80° and 171.81° respectively. The bending of the Ru–Ga–C unit of **4** is significantly different from the linear arrangement seen in  $[\text{Rh}(\text{GaCp}^*)_4(\text{GaCH}_3)][\text{BAR}^F]$  (Rh–Ga–CH<sub>3</sub> 176.1(5)). Apparently, the driving force of the isomerization **4**→**5** correlates with the relaxation of the Ru–Ga–C angle.

To get more insight into the bonding situation of the isomers **4** and **5** DFT calculations were performed<sup>[40]</sup> for the model compounds **4M** and **5M** where Cp\* is replaced by Cp. Geometry optimizations at RI-BP86/def2-SVP of **4M** and **5M** gave bond lengths and angles, which are very similar to the experimental data of **4** and **5**. In particular, the calculated Ga–Ga lengths of **4M** (2.580 Å, exptl: 2.584 Å) and **5M** (2.577 Å, exptl: 2.540 Å) concur quite well with experiment. The calculations show that isomer **5M** is 5.76 kcal mol<sup>-1</sup> lower in energy than **4M**, in agreement with the experimental evidence that **4** is the kinetic and **5** the thermodynamic product. We analyzed the bonding situation in **4M** and **5M** by using the AIM method<sup>[41]</sup> to understand the nature of the Ga–

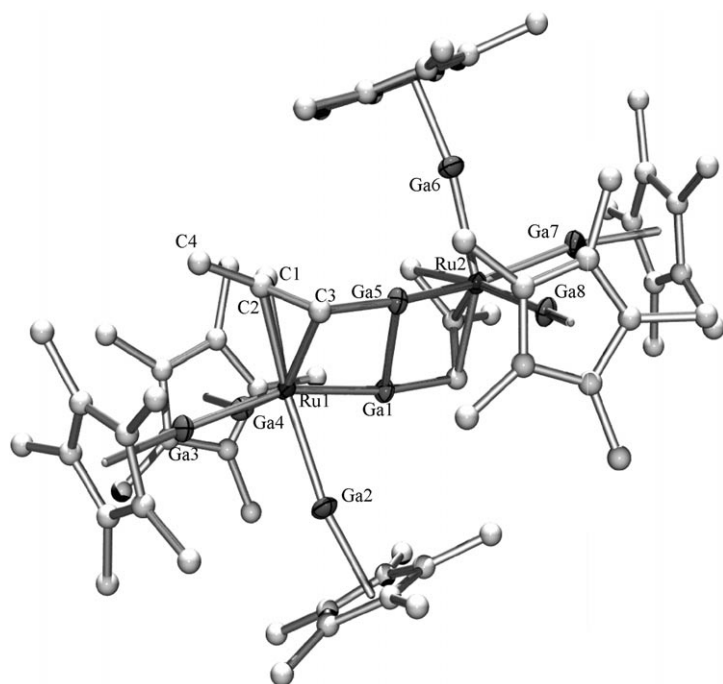


Figure 5. Molecular structure of the cationic part of **5** in the solid state as determined by X-ray single crystal diffraction (thermal ellipsoids are shown at the 50% probability level, hydrogen atoms have been omitted for clarity).

Ga interactions. Figure 3 displays the results of the topological analysis of **4M**. There are bond paths and bond-critical points for Ga–C and Ga–Ru as expected, but surprisingly there is also a bond path and a bond-critical point for the Ga–Ga interactions. The calculated energy density at the Ga–Ga bond-critical point  $H(r_b) = -0.014 \text{ Hartree } \text{Å}^{-3}$  suggests a closed-shell interaction with only weak covalent bonding contributions.<sup>[42]</sup> However, the calculated values for the Ga–Ru bond ( $H(r_b) = -0.030 \text{ Hartree } \text{Å}^{-3}$ ) and the Ga–C bond ( $H(r_b) = -0.051 \text{ Hartree } \text{Å}^{-3}$ ) indicate that the covalent contributions in the latter bonds are not much higher. The results for **5M** are not very different from **4M** and, therefore, are not given here. We conclude that there is indeed a weak attractive Ga–Ga interaction in both compounds **4** and its isomer **5** (Figure 6)

**The reaction of Ga<sup>+</sup> with [Ru(PCy<sub>3</sub>)<sub>2</sub>(GaCp\*)<sub>2</sub>(H)<sub>2</sub>] (**2**):** Protonation of the closed shell 18 VE complex **2** by  $[\text{H}(\text{OEt}_2)_2][\text{BAr}^F]$  leads to unselective decomposition of the starting material with crystals of  $[\text{HPCy}_3][\text{BAr}^F]$  as the only isolable decomposition product. Remarkably, the analogous treatment of **2** with one molar equivalent of  $[\text{Ga}_2\text{Cp}^*][\text{BAr}^F]$  selectively gives the ionic compound  $[\text{Ru}(\text{PCy}_3)_2(\text{GaCp}^*)_2(\text{Ga})][\text{BAr}^F]$  (**6**) under evolution of H<sub>2</sub> (Scheme 2), which is clearly visible on mixing the starting materials. The <sup>1</sup>H NMR of **6** does not show any signals in the typical range of Ru–H groups, whereas the typical region for Ga–H groups is covered by the broad PCy<sub>3</sub> signals. However, also the IR spectrum does not exhibit any bands in the typical

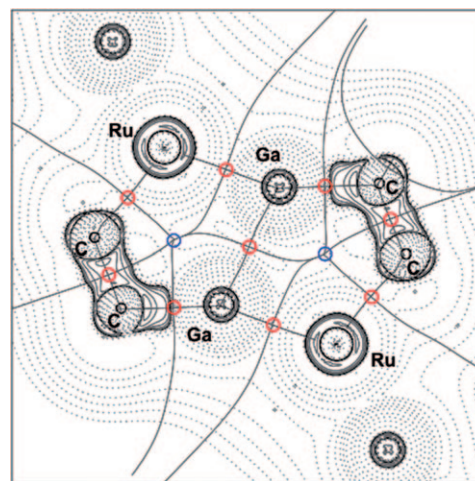
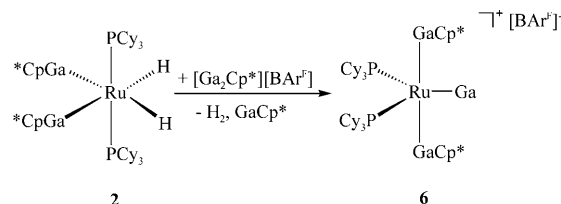


Figure 6. Laplacian  $\nabla^2\rho(r)$  of **4M**. Solid lines indicate areas of charge concentration ( $\nabla^2\rho(r) < 0$ ) while dashed lines show areas of charge depletion ( $\nabla^2\rho(r) > 0$ ). The thick solid lines connecting the atomic nuclei are the bond paths. The thick solid lines separating the atomic basins indicate the zero-flux surfaces crossing the molecular plane. Red circles indicate bond-critical points and blue circles show ring critical points.



Scheme 2. Reaction of **2** with  $[\text{Ga}_2\text{Cp}^*][\text{BAr}^F]$  in fluorobenzene solution.

region of Ga–H or Ru–H stretching frequencies. Upon slow diffusion of *n*-hexane into a fluorobenzene solution of **6** at room temperature, colorless single crystals of **6** are obtained. The cation of **6** exhibits a slightly distorted trigonal-bipyramidal structure with the Ga<sup>+</sup> ligand in an equatorial position (Figure 7).

Both GaCp\* ligands now occupy the axial positions of a heavily distorted trigonal bipyramidal coordination sphere around the Ru centre with an angle Ga1–Ru–Ga2 of 157.94(3)°. In contrast to compound **2** the bulky PCy<sub>3</sub> groups move towards each other into equatorial positions with an angle P1–Ru–P2 of 145.58(4)°. Probably as a result of this *cis* coordination of the phosphine ligands, the Ru–P bond lengths are slightly elongated in comparison to the starting complex **2** (2.3286 Å in **2** versus an average of 2.3719 Å in **6**). The GaCp\* ligands are significantly bent towards the terminal Ga<sup>+</sup> ligand, and the Ga3–Ru–Ga1 and Ga3–Ru–Ga2 angles are closer to 80° than 90°. The Ru–GaCp\* bond lengths average to 2.4236 Å and are thus comparable to those of **2** (2.4017 Å). The Ga–Ga lengths are 2.994(2) Å and 3.0148(8) Å respectively. In comparison with the Ga–Ga interactions of **3** and **5** this lengths are quite long and weak bonding interactions in the Ga<sup>+</sup>/GaCp\* pairs are unlikely.

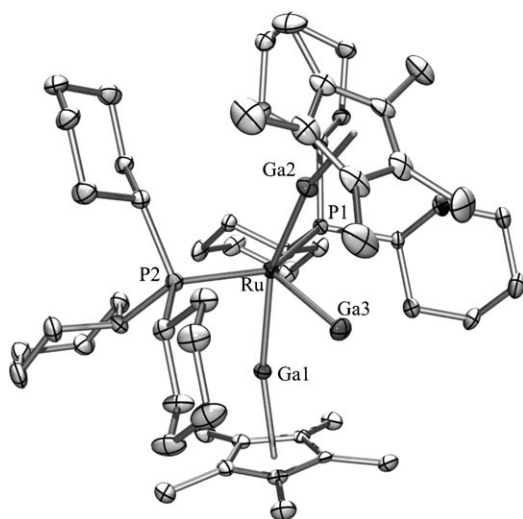


Figure 7. Molecular structure of the cationic part of **6** in the solid state as determined by X-ray single crystal diffraction (thermal ellipsoids are shown at the 50% probability level, hydrogen atoms have been omitted for clarity).

Most interestingly, the bond length of the ruthenium atom to the naked  $\text{Ga}^+$  ion of 2.300(2) Å (Ru–Ga3) is shortened by more than 5% with respect to the Ru–GaCp\* bonds (e.g., Ru–Ga1 = 2.4206(6) Å). Notably, this Ru– $\text{Ga}^+$  bond is the shortest Ru–Ga contact known to date. The cation of **6** could formally be described as a 16e fragment  $[\text{Ru}(\text{PCy}_3)_2(\text{GaCp}^*)_2]^+$ , which is electronically saturated by the donation of the remaining electron pair of  $\text{Ga}^+$  to yield a complex  $[(\text{Ga})\text{Ru}(\text{PCy}_3)_2(\text{GaCp}^*)_2]^+$  with a formal 18e count, but this would be a wrong interpretation of the situation. It was shown by a detailed bonding analysis of the related platinum cations  $[(\text{Ga})\text{Pt}(\text{GaCp})_n]^+$  ( $n = 3, 4$ ) based on DFT calculations that the  $\text{Ga}^+$  ligand exhibits no Lewis basic properties at all, but acts as strong  $\sigma$  and  $\pi$  acceptor, only.<sup>[12]</sup> This is particularly interesting in case of the formally unsaturated 16e platinum complex  $[(\text{Ga})\text{Pt}(\text{GaCp})_3]^+$ , which is of immediate relevance for our discussion of  $[(\text{Ga})\text{Ru}(\text{PCy}_3)_2(\text{GaCp}^*)_2]^+$ . The electron pair of  $\text{Ga}^+$  possesses mainly s character and does not participate in coordinative bonding. The energy decomposition analysis of  $[(\text{Ga})\text{Pt}(\text{GaCp})_n]^+$  showed that the partitioning of the  $\Delta E_{\text{orb}}$  term into the contributions of the  $\sigma$  and  $\pi$  orbitals reveals strong  $\text{E}^+ \text{--Pt} \pi$  interactions leading to a  $\text{Ga}^+ \text{--Pt} \pi$  bonding with nearly the same strength as the  $\text{Ga}^+ \text{--Pt} \sigma$  bonding. Note, that the  $d^8$  Ru center of the fragment  $[\text{Ru}(\text{PCy}_3)_2(\text{GaCp}^*)_2]$  is supposedly even more basic as compared with the platinum centre of  $[\text{Pt}(\text{GaCp})_3]^+$ . This reasoning explains the very short Ru–Ga3 bond length of 2.302(2) Å. There is as strong  $\sigma/\pi$  back donation of the basic ruthenium atom to the very good  $\sigma/\pi$  acceptor ligand  $\text{Ga}^+$ .

## Conclusion

The key messages of the above presented results can be summarized in the following way. First, an attack of carbon nucleophiles at the electrophilic ion  $\text{Ga}^+$  yields an RGa species which expectedly “switches on” the free electron pair of  $\text{Ga}^+$ , that is, the electrophilic  $\text{Ga}^+$  is converted to a basic GaR. This results in the coordination of the monovalent RGa unit to an adjacent Ru centre and finally leads to dimerization as shown by the reactions of Scheme 1 and the compounds **3–5**. Second and more unexpectedly: even metal coordinated, and thus trivalent RGa units, can weakly bind to each other through closed-shell interactions. This effect appears to be important enough to favor the discrete dimeric structures of **4** and **5** over the possible alternative of a polymeric chain. Finally, compound **6** represents just the second example of a complex featuring a naked  $\text{Ga}^+$  coordinating to a transition metal in a terminal fashion. The rather basic  $\text{Ru}^0 d^8$  metal center and the strong  $\sigma/\pi$ -acceptor ligand properties favor an extremely short Ru–Ga length well in line with previous findings on related platinum complexes such as  $[(\text{Ga})\text{Pt}(\text{GaCp}^*)_4]$ .<sup>[12]</sup> Although the exact mechanism of the reaction of  $[\text{Ru}(\text{PCy}_3)_2(\text{GaCp}^*)_2(\text{H})_2]$  (**2**) with the  $\text{Ga}^+$  transfer reagent  $[\text{Ga}_2\text{Cp}^*][\text{BAR}^F]$ , which yields **6** is unknown and no intermediates were detectable by in situ NMR spectroscopy, it may be reasonable to assume that the primary step of this reaction is an insertion of  $\text{Ga}^+$  into a Ru–H bond. This would give an intermediate featuring one more acidic Ru–H and one more basic Ga–H unit. A subsequent polar intra- or intermolecular reaction would lead to  $\text{H}_2$  elimination and formation of the final product.<sup>[45]</sup> By presenting this speculative explanation of the formation of **6** we like to point out that transition metal coordinated GaH species are still unknown and remain a challenge for synthesis.<sup>[17]</sup>

## Experimental Section

**General considerations:** All manipulations were carried out in an atmosphere of purified argon using standard Schlenk and glove box techniques. The solvents were dried using an mBraun Solvent Purification System. The final  $\text{H}_2\text{O}$  content in all solvents was checked by Karl–Fischer titration and did not exceed 5 ppm.  $[\text{Ga}_2\text{Cp}^*][\text{BAR}^F]$ ,<sup>[12]</sup>  $\text{GaCp}^*$ ,<sup>[43]</sup>  $[\text{Ru}(\eta^3\text{-CH}_2\text{CMeCH}_2)_2(\eta^4\text{-COD})]$ <sup>[21]</sup> as well as the hydride complex  $[\text{Ru}(\text{PCy}_3)_2(\text{H})_2(\text{H})_2]$ <sup>[24]</sup> were prepared according to literature methods. Elemental analyses of all compounds were performed at the Laboratory for Microanalytics of the University of Essen (EA 1110 CHNS-O Carlo Erba Instruments). NMR spectra were recorded on a Bruker Avance DPX-250 spectrometer ( $^1\text{H}$  at 250.1 MHz;  $^{13}\text{C}$  at 62.9 MHz) in  $\text{C}_6\text{D}_6$  298 K unless otherwise stated. Chemical shifts are given relative to TMS and were referenced to the solvent resonances as internal standards. All crystal structures were measured on an Oxford Excalibur diffractometer. The structures were solved by direct methods using SHELXS-97 and refined against  $F^2$  on all data by full-matrix least-squares with SHELXL-97.<sup>[44]</sup> Details of the structure determinations of products **1–6** are given in Table S1. CCDC 693098 (**1**), 693099 (**2**), 693100 (**3**), 693101 (**4**), 693102 (**5**) and 693103 (**6**) contain the supplementary crystallographic data for this paper. These data can be obtained free of charge from The Cam-

bridge Crystallographic Data Centre via [www.ccdc.cam.ac.uk/data\\_request/cif](http://www.ccdc.cam.ac.uk/data_request/cif).

**Preparation of [Ru(GaCp\*)<sub>3</sub>(TMM)] (1):** To a solution of [Ru( $\eta^4$ -COD)( $\eta^3$ -CH<sub>2</sub>CMeCH<sub>2</sub>)<sub>2</sub>] (0.300 g, 0.939 mmol) in toluene (6 mL) GaCp\* (0.616 g, 3.005 mmol) was added. The reaction mixture was stirred for 1 h at 80 °C. The solvent was removed in vacuo and the dark-red residue was washed with a small amount of cold *n*-hexane. The precipitate was dissolved in *n*-hexane and slowly cooled to –30 °C while **1** crystallized in form of pale yellow prisms. Yield: 0.448 g yellow crystals (62%). <sup>1</sup>H NMR (C<sub>6</sub>D<sub>6</sub>):  $\delta_{\text{H}}=1.89$  (s, 45H; GaCp\*), 1.76 ppm (s, 6H; CH<sub>2</sub>); <sup>13</sup>C{<sup>1</sup>H} NMR (C<sub>6</sub>D<sub>6</sub>):  $\delta_{\text{C}}=113.5$  (C<sub>5</sub>Me<sub>3</sub>), 84.1 (C<sub>centr</sub>, TMM), 24.5 (CH<sub>2</sub>, TMM), 10.2 ppm (C<sub>5</sub>Me<sub>3</sub>); elemental analysis calcd (%) for C<sub>34</sub>H<sub>51</sub>Ga<sub>3</sub>Ru: C 53.03, H 6.68; found: C 52.14, H 6.54.

**Preparation of [Ru(PCy<sub>3</sub>)<sub>2</sub>(GaCp\*)<sub>2</sub>(H)<sub>2</sub>] (2):** To a solution of [Ru(PCy<sub>3</sub>)<sub>2</sub>(H<sub>2</sub>)<sub>2</sub>(H)<sub>2</sub>] (0.300 g, 0.449 mmol) in hexane (6 mL) GaCp\* (0.203 g, 0.988 mmol) was slowly added at room temperature. The reaction mixture was stirred for 30 min at 60 °C, then all volatiles were removed in vacuo. The bright yellow residue was redissolved in pentane and slowly cooled to –30 °C while **2** crystallized in form of colorless needles. Yield: 0.405 g (84%). <sup>1</sup>H NMR (C<sub>6</sub>D<sub>6</sub>):  $\delta_{\text{H}}=2.07$  (s, 30H; GaCp\*), 1.63 (s, 66H; PCy<sub>3</sub>), –12.74 (triplet, <sup>2</sup>J<sub>(P-H)}=26.31 Hz, 2H); <sup>13</sup>C{<sup>1</sup>H} NMR (C<sub>6</sub>D<sub>6</sub>):  $\delta_{\text{C}}=113.5$  (C<sub>5</sub>Me<sub>3</sub>), 42.6 (br, PCy<sub>3</sub>), 39.4 (br, PCy<sub>3</sub>), 32.4 (br, PCy<sub>3</sub>), 31.2 (br, PCy<sub>3</sub>), 29.4 (br, PCy<sub>3</sub>), 28.5 (br, PCy<sub>3</sub>), 27.6 (s, PCy<sub>3</sub>), 27.3 (s, PCy<sub>3</sub>), 27.1 (s, PCy<sub>3</sub>), 26.9 (s, PCy<sub>3</sub>), 26.5 (s, PCy<sub>3</sub>), 10.8 (C<sub>5</sub>Me<sub>3</sub>); <sup>31</sup>P{<sup>1</sup>H} NMR (C<sub>6</sub>D<sub>6</sub>, 298 K, 101.25 MHz):  $\delta_{\text{P}}=87.04$  (s); IR (Nujol):  $\tilde{\nu}=2026$  and  $2002$  cm<sup>–1</sup> (vs, Ru–H); elemental analysis calcd (%) for C<sub>35</sub>H<sub>96</sub>Ga<sub>2</sub>P<sub>2</sub>Ru: C 62.33, H 9.13; found: C 62.02, H 8.74.</sub>

**Preparation of [Ru(GaCp\*)<sub>4</sub>( $\eta^3$ -CH<sub>2</sub>)<sub>2</sub>C(CH<sub>3</sub>)] [BAR<sup>F</sup>] (3):** After a Schlenk tube was charged with a pure crystalline sample of **1** (0.300 g, 0.390 mmol) and [H(OEt<sub>2</sub>)<sub>2</sub>] [BAR<sup>F</sup>] (0.394 g, 0.390 mmol), fluorobenzene was added at –30 °C. The reaction mixture was stirred for 2 h at room temperature. All volatiles were removed in vacuo and the pale orange residue was washed with hexane (3 × 5 mL). The residue was dissolved in fluorobenzene and the product was crystallized by slow diffusion of *n*-hexane into this solution. Yield: 0.423 g orange crystals (59%). <sup>1</sup>H NMR ([D<sub>8</sub>]THF):  $\delta_{\text{H}}=7.80$  (s, 8H; BAR<sup>F</sup>), 7.58 (s, 4H; BAR<sup>F</sup>), 2.52 (t, <sup>3</sup>J<sub>(H-H)}=1.22 Hz, 2H; syn-CH<sub>2</sub>), 2.29 (t, 2H; <sup>3</sup>J<sub>(H-H)}=1.22 Hz, anti-CH<sub>2</sub>), 2.11 (s, 3H; CH<sub>3</sub>), 2.01 ppm (s, 60H; GaCp\*); <sup>13</sup>C{<sup>1</sup>H} NMR ([D<sub>8</sub>]THF):  $\delta_{\text{C}}=162.8$  (q, J=49.8 Hz, [BAR<sup>F</sup>]), 135.6 ([BAR<sup>F</sup>]), 130.0 (q, J=34.4 Hz, [BAR<sup>F</sup>]), 125.5 (q, J=27.2 Hz, [BAR<sup>F</sup>]), 118.2 ([BAR<sup>F</sup>]) 116.5 (C<sub>5</sub>Me<sub>3</sub>), 92.9 (C, methylallyl) 68.2 (CH<sub>2</sub>, methylallyl), 19.5 (CH<sub>3</sub>, methylallyl), 10.9 ppm (C<sub>5</sub>Me<sub>3</sub>); elemental analysis calcd (%) for C<sub>76</sub>H<sub>79</sub>BF<sub>24</sub>Ga<sub>4</sub>Ru: C 49.63, H 4.33; found: C 50.39, H 3.98.</sub></sub>

**Preparation of [[Ru(GaCp\*)<sub>3</sub>( $\eta^3$ -CH<sub>2</sub>)<sub>2</sub>C(CH<sub>2</sub>( $\mu$ -Ga))]<sub>2</sub>] [BAR<sup>F</sup>]<sub>2</sub> (4):** After a Schlenk tube was charged with a pure crystalline sample of **1** (0.300 g, 0.390 mmol) and [Ga<sub>2</sub>Cp\*] [BAR<sup>F</sup>] (0.443 g, 0.390 mmol), fluorobenzene was added at room temperature. The reaction mixture was stirred for 30 min at room temperature. All volatiles were removed in vacuo and the dark-red residue was washed with hexane (3 × 5 mL). The residue was dissolved in fluorobenzene and the product was crystallized by slow diffusion of *n*-hexane into this solution. Yield: 0.531 g dark-red crystals (80%). The <sup>1</sup>H NMR spectra in CD<sub>2</sub>Cl<sub>2</sub> or fluorobenzene solution is unexpectedly complicated, probably a result of a fluxional processes or parallel equilibria. However, it seems to be possible to assign the main signals to the expected structure (vide infra). Variable temperature NMR measurements are not possible, owing to the fast isomerization of the complex as well as its marked insolubility in organic solvents. <sup>1</sup>H NMR (CD<sub>2</sub>Cl<sub>2</sub>):  $\delta_{\text{H}}=7.73$  (s, 8H; BAR<sup>F</sup>), 7.56 (s, 4H; BAR<sup>F</sup>), 2.44 (br, 4H), 2.28 (br, 4H), 2.25 (4H), 2.04 (s, 30H), 1.94 ppm (60H); elemental analysis calcd (%) for C<sub>76</sub>H<sub>79</sub>BF<sub>24</sub>Ga<sub>4</sub>Ru: C 46.55, H 3.73; found: C 46.31, H 3.34;

**Preparation of [[Ru(GaCp\*)<sub>3</sub>( $\eta^3$ -CH<sub>2</sub>)(CH( $\mu$ -Ga)(CH<sub>3</sub>))]<sub>2</sub>] [BAR<sup>F</sup>]<sub>2</sub> (5):** A solution of a freshly prepared sample of **4** (0.300 g, 0.088 mmol) was refluxed in fluorobenzene for 1 h. After removal of all volatiles in vacuo, the pale yellow residue was washed with hexane (3 × 5 mL). The residue was dissolved in fluorobenzene and the product was crystallized by slow diffusion of *n*-hexane into this solution. Yield: 0.273 g yellow crystals (91%). <sup>1</sup>H NMR (CD<sub>2</sub>Cl<sub>2</sub>):  $\delta_{\text{H}}=7.73$  (s, 16H; BAR<sup>F</sup>), 7.56 (s, 8H;

BAR<sup>F</sup>), 5.16 (d, <sup>3</sup>J<sub>(H-H)}=3.04 Hz, approx. 2H; syn-CH<sub>2</sub>), 2.45 ppm (s, 6H; CH<sub>3</sub>), 1.98 (s, 90H; GaCp\*), 1.68 (t, 2H; <sup>3</sup>J<sub>(H-H)}=3.22 Hz, anti-CH<sub>2</sub>), –2.09 ppm (d, <sup>3</sup>J<sub>(H-H)}=3.41 Hz, 2H); <sup>13</sup>C{<sup>1</sup>H} NMR (CD<sub>2</sub>Cl<sub>2</sub>):  $\delta_{\text{C}}=164.6$  (q, J=49.8 Hz, [BAR<sup>F</sup>]), 137.7 ([BAR<sup>F</sup>]), 131.7 (q, J=31.5 Hz, [BAR<sup>F</sup>]), 127.5 (q, J=27.2 Hz, [BAR<sup>F</sup>]), 120.3 ([BAR<sup>F</sup>]) 118.8 (broad, C<sub>5</sub>Me<sub>3</sub>), 106.7 (gallallyl), 104.8 (gallallyl), 37.8 (gallallyl), 23.4 (CH<sub>3</sub>, gallallyl), 13.4 ppm (C<sub>5</sub>Me<sub>3</sub>); elemental analysis calcd (%) for C<sub>76</sub>H<sub>79</sub>BF<sub>24</sub>Ga<sub>4</sub>Ru: C 46.55, H 3.73; found: C 46.51, H 3.52.</sub></sub></sub>

**Preparation of [Ru(PCy<sub>3</sub>)<sub>2</sub>(GaCp\*)<sub>2</sub>(Ga)] [BAR<sup>F</sup>] (6):** A sample of **2** (0.300 g, 0.283 mmol) in 4 mL fluorobenzene was treated with a fluorobenzene solution (3 mL) of [Ga<sub>2</sub>Cp\*] [BAR<sup>F</sup>] (0.322 g, 0.283 mmol) at room temperature. The reaction mixture was stirred for 1 h at room temperature. The solvent was reduced in vacuo to about 2 mL, and the product was precipitated by addition of *n*-hexane to give a colorless crystalline solid. The solvent was removed by filtration, the residue washed with hexane (2 × 2 mL), and dried in vacuo. Recrystallization of the crude product by slow diffusion of hexane into a fluorobenzene solution gave well formed needle-shaped crystals. Yield: 0.440 g (78%). <sup>1</sup>H NMR (C<sub>6</sub>H<sub>5</sub>F/C<sub>6</sub>D<sub>6</sub>, 10:1):  $\delta_{\text{H}}=8.32$  (s, 8H; BAR<sup>F</sup>), 7.67 (s, 4H; BAR<sup>F</sup>), 1.97 (s, 30H; GaCp\*), 1.36 (s, 66H; PCy<sub>3</sub>). <sup>31</sup>P NMR (C<sub>6</sub>H<sub>5</sub>F/C<sub>6</sub>D<sub>6</sub>, 10:1):  $\delta_{\text{P}}=66.9$  (s, PCy<sub>3</sub>); <sup>13</sup>C{<sup>1</sup>H} NMR (CD<sub>2</sub>Cl<sub>2</sub> 10:1):  $\delta_{\text{C}}=162.2$  (q, J=49.2 Hz, [BAR<sup>F</sup>]), 135.2 ([BAR<sup>F</sup>]), 130.4 (q, J=34.1 Hz, [BAR<sup>F</sup>]), 125.9 (q, J=27.2 Hz, [BAR<sup>F</sup>]), 118.3 ([BAR<sup>F</sup>]) 119.5 (C<sub>5</sub>Me<sub>3</sub>), 36.8 (s, PCy<sub>3</sub>), 33.9 (s, PCy<sub>3</sub>), 31.8 (s, PCy<sub>3</sub>), 31.4 (s, PCy<sub>3</sub>), 30.6 (s, PCy<sub>3</sub>), 30.5 (s, PCy<sub>3</sub>), 29.3 (s, PCy<sub>3</sub>), 28.6 (s, PCy<sub>3</sub>), 28.4 (s, PCy<sub>3</sub>), 27.1 (s, PCy<sub>3</sub>), 13.2 ppm (C<sub>5</sub>Me<sub>3</sub>); elemental analysis calcd (%) C<sub>87</sub>H<sub>106</sub>BF<sub>24</sub>Ga<sub>3</sub>P<sub>2</sub>Ru: C 52.49, H 5.37; found: C 52.00, H 6.08.

## Acknowledgement

T.C. is grateful for a stipend by the Fonds of the Chemical Industry Germany and for support by the Ruhr University Research School.

- [1] C. Jones, P. C. Junk, J. A. Platts, A. Stasch, *J. Am. Chem. Soc.* **2006**, *128*, 2206–2207.
- [2] R. J. Baker, C. Jones, J. A. Platts, *J. Am. Chem. Soc.* **2003**, *125*, 10534–10535.
- [3] R. J. Baker, C. Jones, M. Klothe, J. A. Platts, *Angew. Chem.* **2003**, *115*, 2764–2767; *Angew. Chem. Int. Ed.* **2003**, *42*, 2660–2663.
- [4] R. J. Baker, R. D. Farley, C. Jones, M. Klothe, D. M. Murphy, *J. Chem. Soc. Dalton Trans.* **2002**, 3844–3850.
- [5] M. C. Kuchta, J. B. Bonanno, G. Parkin, *J. Am. Chem. Soc.* **1996**, *118*, 10914–10915.
- [6] N. J. Hardman, B. E. Eichler, P. P. Power, *Chem. Commun.* **2000**, 1991–1992.
- [7] N. J. Hardman, R. J. Wright, A. D. Phillips, P. P. Power, *J. Am. Chem. Soc.* **2003**, *125*, 2667–2679.
- [8] a) E. S. Schmidt, A. Jockisch, H. Schmidbaur, *J. Am. Chem. Soc.* **1999**, *121*, 9758–9759; b) P. Jutz, B. Neumann, L. O. Schebaum, A. Stammer, H.-G. Stammer, *Organometallics* **1999**, *18*, 4462–4464; c) H. Braunschweig, C. Kollann, D. Rais, *Angew. Chem.* **2006**, *118*, 5380–5400; *Angew. Chem. Int. Ed.* **2006**, *45*, 5254–5274; d) C. Dohmeier, D. Loos, H. Schnoekel, *Angew. Chem.* **1996**, *108*, 141–161; *Angew. Chem. Int. Ed. Engl.* **1996**, *35*, 129–149; e) W. Uhl, M. Pohlmann, R. Wartchow, *Angew. Chem.* **1998**, *110*, 1007–1009; *Angew. Chem. Int. Ed.* **1998**, *37*, 961–963.
- [9] a) N. D. Coombs, W. Clegg, A. L. Thompson, D. J. Willock, S. Aldridge, *J. Am. Chem. Soc.* **2008**, *130*, 5449–5451; b) H.-J. Himmel, G. Linti, *Angew. Chem. Int. Ed.* **2008**, *47*, 6326–6328.
- [10] T. Cadenbach, C. Gemel, D. Zacher, R. A. Fischer, *Angew. Chem. Int. Ed.* **2008**, *47*, 3438–3441.
- [11] a) B. Buchin, C. Gemel, T. Cadenbach, R. Schmid, R. A. Fischer, *Angew. Chem.* **2006**, *118*, 1091–1093; *Angew. Chem. Int. Ed.* **2006**, *45*, 1074–1076; b) I. Fernandez, E. Cerpa, G. Merino, G. Frenking,

- Organometallics* **2008**, *27*, 1006; c) for [In<sub>2</sub>Cp\*] see: A. H. Cowley, *Chem. Commun.* **2004**, 2369.
- [12] B. Buchin, C. Gemel, T. Cadenbach, I. Fernandez, G. Frenking, R. A. Fischer, *Angew. Chem.* **2006**, *118*, 5331–5334; *Angew. Chem. Int. Ed.* **2006**, *45*, 5207–5210.
- [13] S. Aldridge, *Angew. Chem.* **2006**, *118*, 8275–8277; *Angew. Chem. Int. Ed.* **2006**, *45*, 8097–8099.
- [14] B. Buchin, *Diploma thesis* **2005**.
- [15] T. Cadenbach, C. Gemel, R. Schmid, R. A. Fischer, *J. Am. Chem. Soc.* **2005**, *127*, 17068–17078.
- [16] a) M. Cokoja, C. Gemel, T. Steinke, F. Schroeder, R. A. Fischer, *Dalton Trans.* **2005**, 44–54; b) T. Steinke, C. Gemel, M. Cokoja, M. Winter, R. A. Fischer, *Dalton Trans.* **2005**, 55–62.
- [17] A. Kempter, C. Gemel, T. Cadenbach, R. A. Fischer, *Inorg. Chem.* **2007**, *46*, 9481.
- [18] T. Steinke, C. Gemel, M. Cokoja, M. Winter, R. A. Fischer, *Chem. Commun.* **2003**, 1066–1067.
- [19] B. Buchin, C. Gemel, A. Kempter, T. Cadenbach, R. A. Fischer, *Inorg. Chim. Acta* **2006**, *359*, 4833–4839.
- [20] G. Prabusankar, A. Kempter, C. Gemel, R. A. Fischer, *Angew. Chem.* **2008**, *120*, 7344–7347; *Angew. Chem. Int. Ed.* **2008**, *47*, 7234–7237.
- [21] K. S. MacFarlane, S. J. Rettig, Z. Liu, B. R. James, *J. Organomet. Chem.* **1998**, *557*, 213–219.
- [22] M. D. Jones, R. D. W. Kemmitt, A. W. G. Platt, *J. Chem. Soc. Dalton Trans.* **1986**, 1411–1418.
- [23] K. McNeill, R. A. Andersen, R. G. Bergman, *J. Am. Chem. Soc.* **1997**, *119*, 11244–11254.
- [24] A. F. Borowski, S. Sabo-Etienne, M. L. Christ, B. Donnadiu, B. Chaudret, *Organometallics* **1996**, *15*, 1427–1434.
- [25] T. Cadenbach, T. Bollermann, C. Gemel, R. A. Fischer, *Dalton Trans.* **2008**, in press.
- [26] T. Steinke, M. Cokoja, C. Gemel, A. Kempter, A. Krapp, G. Frenking, U. Zenneck, R. A. Fischer, *Angew. Chem.* **2005**, *117*, 3003–3007; *Angew. Chem. Int. Ed.* **2005**, *44*, 2943–2946.
- [27] M. Ohashi, K. Matsubara, T. Iizuka, H. Suzuki, *Angew. Chem.* **2003**, *115*, 967–970; *Angew. Chem. Int. Ed.* **2003**, *42*, 937–940.
- [28] R. H. Crabtree, D. G. Hamilton, *J. Am. Chem. Soc.* **1986**, *108*, 3124–3125.
- [29] G. J. Kubas, *Acc. Chem. Res.* **1988**, *21*, 120–128.
- [30] M. Grellier, L. Vendier, B. Chaudret, A. Albinati, S. Rizzato, S. Mason, S. Sabo-Etienne, *J. Am. Chem. Soc.* **2005**, *127*, 17592–17593.
- [31] J. Eckert, C. M. Jensen, T. F. Koetzle, T. L. Husebo, J. Nicol, P. Wu, *J. Am. Chem. Soc.* **1995**, *117*, 7271–7272.
- [32] T. Braun, G. Muench, B. Windmueller, O. Gevert, M. Laubender, H. Werner, *Chem. Eur. J.* **2003**, *9*, 2516–2530.
- [33] V. Cadierno, P. Crochet, J. Diez, S. E. Garcia-Garrido, J. Gimeno, S. Garcia-Granda, *Organometallics* **2003**, *22*, 5226–5234.
- [34] T. Kondo, H. Ono, N. Satake, T.-a. Mitsudo, Y. Watanabe, *Organometallics* **1995**, *14*, 1945–1953.
- [35] M. D. Mbaye, B. Demerseman, J.-L. Renaud, L. Toupet, C. Bruneau, *Angew. Chem.* **2003**, *115*, 5220–5222; *Angew. Chem. Int. Ed.* **2003**, *42*, 5066–5068.
- [36] H. Sasabe, S. Nakanishi, T. Takata, *Inorg. Chem. Commun.* **2003**, *4*, 1140–1143.
- [37] P. Xue, S. Bi, H. H. Y. Sung, I. D. Williams, Z. Lin, G. Jia, *Organometallics* **2004**, *23*, 4735–4743.
- [38] N. Wiberg, K. Amelunxen, H. W. Lerner, H. Noth, W. Ponikwar, H. Schwenk, *J. Organomet. Chem.* **1999**, *574*, 246–251.
- [39] X. He, R. A. Bartlett, M. M. Olmstead, K. Ruhlandt-Senge, B. E. Sturgeon, P. P. Power, *Angew. Chem.* **1993**, *105*, 761–762; *Angew. Chem. Int. Ed. Engl.* **1993**, *32*, 717–719.
- [40] DFT calculations were carried out at RI-BP86/def2-SVP, a) A. D. Becke, *Phys. Rev. A* **1988**, *38*, 3098; b) J. P. Perdew, *Phys. Rev. B* **1986**, *33*, 8822; c) F. Weigend, R. Alhrichs, *Phys. Chem. Chem. Phys.* **2005**, *7*, 3297, using TURBOMOLE (v5.90); d) R. Alhrichs, M. Baer, M. Haeser, H. Horn, C. Koelmel, *Chem. Phys. Lett.* **1989**, *162*, 165.
- [41] R. F. W. Bader, *Atoms in Molecules. A Quantum Theory*, Oxford University Press, Oxford, **1990**.
- [42] D. Cremer, E. Kraka, *Angew. Chem. Int. Ed. Engl.* **1984**, *23*, 62.
- [43] a) P. Jutzi, B. Neumann, G. Reumann, H.-G. Stammer, *Organometallics* **1998**, *17*, 1305–1314; b) P. Jutzi, L. O. Schebaum, *J. Organomet. Chem.* **2002**, *654*, 176–179.
- [44] G. M. Sheldrick, SHELXS-97, Program for the Solution of Crystal Structures, Universität Goettingen, **1997**; G. M. Sheldrick, SHELXL-97, Program for Crystal Structure Refinement, Universität Goettingen, **1997**.
- [45] Preliminary DFT calculations support this hypothetical mechanism. However, detailed computational studies as well as experimental verification is subject of current research and will be reported elsewhere.

Received: July 2, 2008

Published online: October 27, 2008